

Emission of twin jets from a driven matter-wave soliton in a quasi-one-dimensional geometry

Tadej Mežnaršič,* Rok Žitko, Tina Arh, Erik Zupanič, and Peter Jeglič†

Jožef Stefan Institute, Jamova 39, SI-1000 Ljubljana, Slovenia

(Dated: July 28, 2022)

The modulation of the interaction between the atoms in a matter-wave soliton in a quasi-one-dimensional optical trap triggers an emission of correlated atom jets. We characterize the dependence of jet properties on the frequency, amplitude and length of the modulation, and qualitatively reproduce the trends in the mean-field picture with a one-dimensional time-dependent Gross-Pitaevskii equation simulation. High-order jets are observed for sufficiently long pulses, a double-pulse modulation sequence produces consecutive jets, and a multi-pulse sequence may lead to irregular jets at a finite angle to the direction of the channel. Finally, possible number squeezing of the jet pairs is investigated.

Periodic modulation of parameters of a physical system often leads to novel phenomena. Cold-atom systems offer excellent control of the trap geometry and interactions and are therefore extremely suitable for such studies. These range from resonantly exciting quadrupole modes in a trapped Bose-Einstein condensate (BEC) by modulating the interatomic interaction [1], to parametrically amplifying the Faraday waves in a BEC by modulating the trapping potential [2] or the interaction [3], and creating synthetic gauge fields and various topological effects by modulating optical lattices [4]. Harmonic modulation of the interatomic interaction in a BEC stimulates collisions between the atoms and can lead to emission of matter-wave jets, as first observed in a two-dimensional trapping geometry [5]. The emission is preceded by the emergence of strong density waves in the condensate [6]. Intricate angular correlations arise in the two-dimensional case [7], making the interpretation of the involved processes difficult. The attempts at explaining the origin of the jets and their properties have employed a variety of theoretical approaches of different levels of sophistication with varying success [8–10].

In this Letter we present the observation of jets emitted from a matter-wave soliton in quasi-one-dimensional (quasi-1D) geometry. First and second order jets are observed with a single modulation pulse and consecutive jets for a double modulation pulse. For multiple modulation pulses irregular jets appear, seemingly oblivious to the quasi-1D confinement. All stages of the Bose jet emission are captured in a simple model based on the 1D Gross-Pitaevskii equation, giving an insight into the dynamics of density waves that precede the emission. Additionally, the twin-jet number correlations are investigated to determine if the pairs exhibit number squeezing. The absence of complex angular dependence makes these observations much more straightforward than in previous experiments in 2D [5–7].

We start by making a BEC of about 5000-10000 ^{133}Cs atoms in a crossed dipole trap, from which we release it into a channel with radial frequency $\omega_r = 2\pi \cdot 101 \text{ Hz}$ and a weak axial anti-trapping potential with "fre-

quency" $2\pi \cdot 3.33 \text{ Hz}$. Via the broad s -wave Feshbach resonance with zero crossing near 17 G [11] we tune the scattering length from positive (repulsive interaction) to slightly negative (attractive interaction) to obtain a bright matter-wave soliton [12], a nondispersing wave-

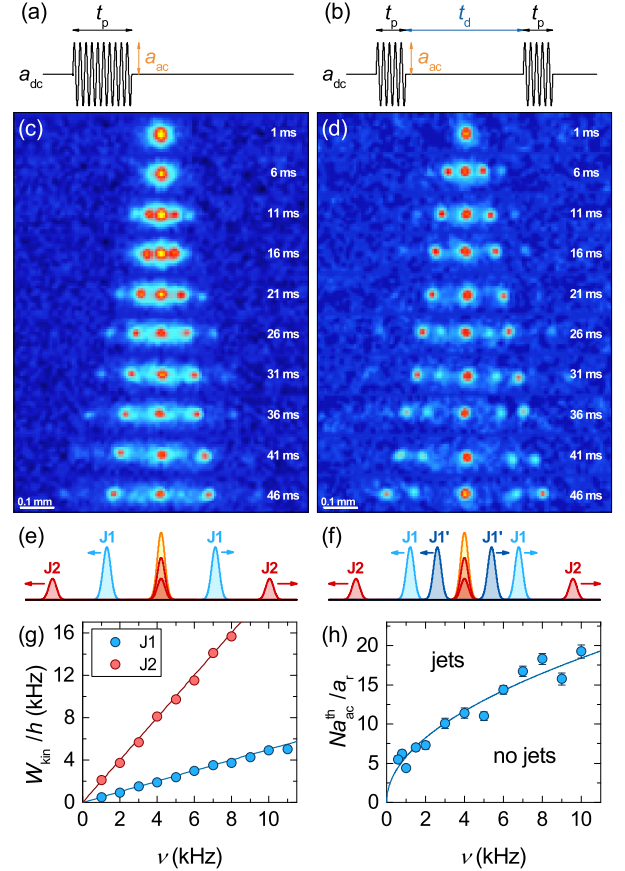


FIG. 1. (a,b) Single- and double-pulse modulation sequences. The time evolution of jets (c) for 2 kHz, $a_{ac} = 52a_0$, $t_p = 11 \text{ ms}$ single-pulse and (d) for 4 kHz, $a_{ac} = 78a_0$, $\{t_p, t_d\} = \{6, 10\} \text{ ms}$ double-pulse modulation sequence (15 ms time-of-flight). (e, f) Schematic representation of the jets in (c, d). (g) Atom kinetic energy dependence on the modulation frequency for J1 and J2 jets. (h) Frequency dependence of the threshold modulation amplitude for jet formation ($t_p = 50 \text{ ms}$).

packet that forms due to the nonlinearity of the interatomic interaction [13–20]. Solitons maintain their density when released into the channel, ensuring stable conditions during the experiments.

After releasing the BEC into the channel we modulate the scattering length for a finite time t_p as $a(t) = a_{dc} + a_{ac} \sin(2\pi\nu t)$, see Fig. 1(a), or we generate pulse-trains, see Fig. 1(b). Here, a_{ac} and ν are the amplitude and the frequency of the modulation, while a_{dc} is the solitonic scattering length. In a typical experiment, modulation frequencies range from 600 Hz to 11 kHz with amplitudes of up to $120a_0$, where a_0 is Bohr radius. The modulation of the interaction triggers the emission of matter-wave jets from the soliton. A typical time evolution for a single pulse is shown in Fig. 1(c). The BEC symmetrically emits two pairs of jets with different velocities. The outer pair (“second-order” jets, J2) is twice as fast as the inner pair (“first-order” jets, J1). Fig. 1(g) shows the frequency dependence of the kinetic energy of the atoms in J1 and J2. Atoms forming J1 have kinetic energy exactly $h\nu/2$, those in J2 exactly $2h\nu$, where h is the Planck constant. From energy and momentum conservation it follows that J2 forms from the atoms in J1, rather than from the atoms in the central BEC, in fact, two J2 jets form from each J1, with half the atoms remaining inside the central cloud with zero velocity [see Fig. 1(e, f)] [21].

In order for the jets to form, the amplitude of the modulation must exceed a threshold value of a_{ac}^{th} , defined in Ref. 5 as the balance between the excitation and escape rates of the ejected atoms. The frequency dependence of the threshold [Fig. 1(h)] follows the square root function, just like in the two-dimensional case [5]. Importantly, the interaction between the atoms depends not only on the scattering length but also on the density of atoms. Therefore, to account for atom number and thus density fluctuations in different experimental runs, the interaction modulation in Fig. 1(h) is given as a dimensionless product Na/a_r , where N is number of atoms in the soliton and $a_r = \sqrt{\hbar/m\omega_r}$ harmonic oscillator length with reduced Planck constant \hbar and atomic mass m . In the double-pulse case we observe that an additional jet J1’ is generated by the second pulse [Fig. 1(d)]. It has the same initial velocity as the first J1. After the second pulse the condensate is too depleted and the threshold cannot be exceeded to create a third “first-order” jet.

For a_{ac} above the threshold, the number of atoms in the jets as a function of the pulse duration t_p first exponentially increases and then slowly saturates. The exponential growth is characteristic for bosonic stimulation [22] and the saturation happens due to the depletion of the central BEC: with decreasing number of atoms in the cloud the frequency of collisions decreases and the jet formation processes gradually become rarer until they completely stop. The ratio between the number of atoms in the fully-formed jets and the total number of

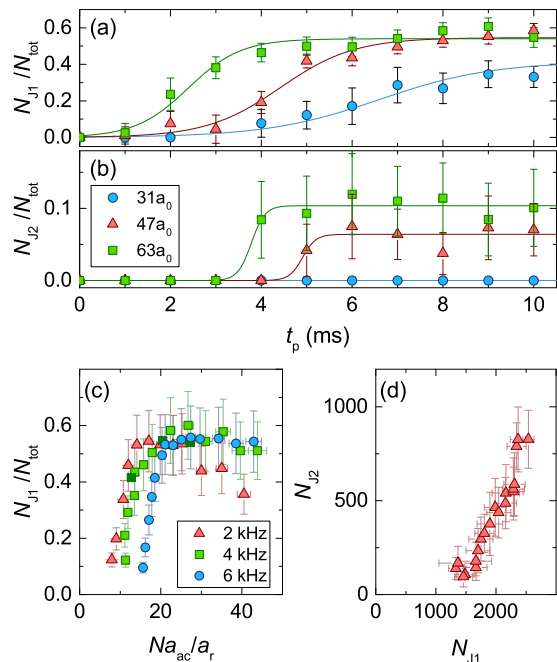


FIG. 2. (a, b) Fraction of atoms in J1 and J2 jets as a function of pulse length for 4 kHz modulation of different amplitudes. The solid lines are $b/[c + \exp(-a \cdot t_p)]$ fits to the data. (c) Modulation amplitude dependence of the saturated number of atoms in J1 jets for 2 kHz, 4 kHz and 6 kHz modulation. The darker green squares mark the measurements shown in (a). (d) Dependence of number of atoms in J2 on the number of atoms in J1, for 1.25 kHz, $a_{ac} = 36a_0$, 11 ms single pulse.

atoms is shown for different modulation amplitudes a_{ac} in Fig. 2(a,b) for J1 and J2, respectively. The number of atoms in jets rises more slowly with increasing t_p and to a lower final value for lower a_{ac} . No atoms are emitted below some threshold value, as clearly observed for J2 for the lowest value of a_{ac} shown. If a_{ac} is increased beyond a certain “optimal” value the saturated number of emitted atoms starts decreasing as seen in Fig. 2(c) for three different frequencies; at higher frequency the optimal a_{ac} is higher. At high amplitudes beyond the optimal value the losses from the condensate increase significantly and we observe a pronounced diffuse background in addition to the central BEC and the jets.

The dependence of the number of atoms in J2 on number of atoms in J1, Fig. 2(d), allows us to determine the minimal number of atoms in J1 required for the formation of J2 at a chosen modulation amplitude. For the case in Fig. 2(d) no J2 are observed while the number of atoms in J1 is under 1300. Above this line the threshold for the formation of J2 is exceeded and the number of atoms rapidly increases. The delay between the formation of J2 and J1 [Fig. 2(a, b)] has the same origin: J2 only form after enough atoms have accumulated in J1 to surpass the threshold.

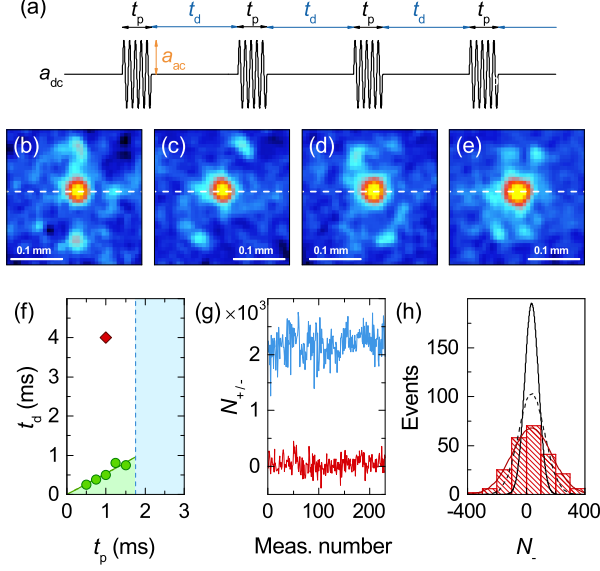


FIG. 3. (a) Multi-pulse train used in the experiments shown in (b-f). (b-e) Jets formed at a finite angle to the direction of the channel (white dashed line), for t_p and t_d marked by the red diamond in (f). (f) Phase diagram for jet formation with 4 kHz, $a_{ac} = 47a_0$ pulse trains. (g) Sum N_+ (blue) and difference N_- (red) of the atom numbers in the left and right J1 jets for 230 consecutive measurements. (h) Histogram of N_- from (g) and a corresponding fit (red), Gaussian distribution with standard deviation $\sqrt{\langle N_+ \rangle}$ (solid black), and Gaussian distribution representing estimated background noise with standard deviation σ_{det} (dashed).

Figs. 2(a, b) indicate that jets cannot form if the modulation pulse is too short. Nevertheless, it is possible to generate jets by exciting the BEC with a train of several short pulses of length t_p separated by time delays t_d , see Fig. 3(a). The total duration of the pulse train is fixed, meaning that there are more pulses in trains with shorter t_p and t_d . From the results one can establish a phase diagram Fig. 3(f). In the blue region the jets are emitted after a single pulse, in the green region after multiple pulses, while in the white region no jets are emitted.

The red diamond in Fig. 3(f) marks a special case where we do not observe the jets along the direction of the channel, but at a finite angle, as shown in Figs. 3(b-e). The angle of these irregular jets appears to be random, and multiple jets can also be observed as shown in Fig. 3(e). They have insufficient energy to escape the confinement potential, thus they oscillate in the channel and can only be observed after an appropriately long time-of-flight (usually 15 ms).

Microscopic processes responsible for the ejection of atoms have been identified to be photon-stimulated two-atom collisions [5]. This can be modeled through Bogoliubov approximation by separating the field operator

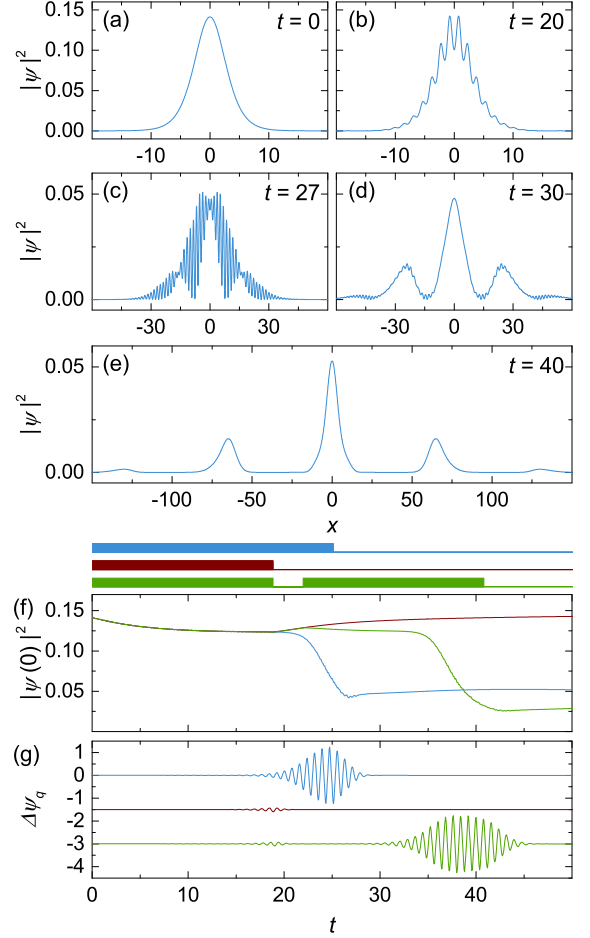


FIG. 4. Simulation. (a-e) snapshots of condensate density during the formation of jets. Please note the changing scales in different panels. The model parameters are $k_{dc} = -0.045$, $k_{ac} = 1.8$, $\omega = 16$, $t_p = 8\pi$. Time-dependence of the central soliton amplitude (f) and density modulation amplitude (g) for the modulation pulse sequences shown above (f) (blue: $t_p = 8\pi$, red: $t_p = 6\pi$ and green: $t_p = 6\pi$, $t_d = \pi$). The red and green curve in (g) are offset for clarity.

into negligibly-depleted condensate and an excited-mode field [5], through more involved methods [8, 10], or by numerically solving the time-dependent Gross-Pitaevskii equation (GPE) [6, 23]. Here we used the latter approach in 1D [24]. We find that all aspects of the problem are captured correctly in this simple picture: the formation of the density modulation and its exponential growth, the emission of the jets (including the formation of the higher-order jets J2), the frequency dependences of density-wave wavelength and kinetic energy of the jets, the existence of various thresholds, as well as the qualitative functional forms of all dependences shown in Figs. 1, 2. We have furthermore studied the time-evolution in the full 3D problem with realistic parameters, confirming the dominant 1D character of the

density-wave and thereby validating the simplified 1D modelling; to fully explore the 3D case further study is required.

Fig. 4(a-e) shows snapshots of the condensate density $n = |\psi(x)|^2$ for a single pulse modulation sequence at five moments: (a) initial state, (b) emerging density-wave, (c) strongly perturbed condensate at the moment of the jet ejection, (d) resulting J1 and J2 jets showing residual density modulation, (e) asymptotic state with one stationary soliton and two pairs of traveling solitons. We also show the time-dependence of the amplitude of the central soliton in Fig. 4(f) and the amplitude of the density modulation in Fig. 4(g) for three different modulation sequences. Interatomic interaction is given as a dimensionless parameter $k = Na/a_r$, modulation frequency as $\omega = 2\pi\nu$, time in units $1/\omega_r$ and distances in units a_r . In the early stages, the BEC slightly changes its shape due to the rectified effect of the modulation [visible as the relaxation of the soliton amplitude up to $t \approx 12$ in panel (f)], and hardly perceptibly expands and contracts as a whole, i.e., the breathing mode is being excited. The density modulation with wave number $q = \sqrt{m\omega/\hbar}$ becomes appreciable for $t \gtrsim 15$. The jets start to form at $t \approx 25$ [blue in (f, g)]. The density-wave amplitude starts to decay when the modulation pulse ends at $t_p = 8\pi$ and eventually the waveforms of both the central peak and the jets J1 and J2 tend toward smooth soliton-like line-shapes (but never reaching the ideal $1/\cosh(x)$ form). If the driving modulation ends prematurely, the density wave disappears, no jets are emitted and the BEC returns to the initial solitonic shape [red in (f, g)]. However, a second driving pulse after a sufficiently short delay can revive the almost extinguished density wave leading to jet emission [green in (f, g)]. These examples give further insight into the boundary between the green and white region in Fig. 3(f). If the delay t_d between the modulation pulses is short, so that the density wave decays only partially, jets are generated (green regions), otherwise they are not (white region). For longer pulse times t_p the density wave amplitude is higher and takes longer to decay. The boundary between the two regions is linear, because growth (during time t_p) and decay (during time t_d) of the modulation both have exponential time dependence.

Because of the momentum conservation during the jet emission process one naturally expects the same number of atoms in the left and right jet (N_L and N_R). Random processes such as interatomic collisions that produce matter-wave jets exhibit Poissonian statistics, which means that the variance of the number of atoms in either jet should be the same as its average over many measurements $\langle N_L \rangle$ ($\langle N_R \rangle$). If the left and right jet were created independently, the sum $N_+ = N_L + N_R$ and difference $N_- = N_L - N_R$ would also have Poissonian distributions with variance $\langle N_+ \rangle$. But because the jets form with pairwise collisions of condensate atoms the number difference

is no longer random and its variance should be below the shot-noise (sub-Poissonian). Accordingly, the conjugate variable N_+ should have a variance larger than shot-noise (super-Poissonian). This is known as number squeezing, which is often a precursor for many-body entanglement [25–29].

Fig. 3(g) shows the number difference between the left and right J1, N_- , and total number in J1, N_+ , over 230 measurements. The standard deviation is well beyond the shot-noise $\sqrt{\langle N_+ \rangle} \approx 47$ in both cases (135 for N_- and 247 for N_+), which we attribute to detection noise which is already larger than the shot-noise at $\sigma_{det} \approx 88$ [see Fig. 3(h) for comparison between different cases]. Even with subtracted σ_{det} the N_- fluctuations are still above $\sqrt{\langle N_+ \rangle}$. Additional contribution to the noise could arise from asymmetric formation of J2 jets, i.e., if more atoms go into second order from the left J1 than from the right J1 or vice versa. On the other hand, N_+ clearly has wider distribution than N_- in Fig. 3(g), suggesting number squeezing even though the sub-Poissonian distribution cannot be directly proven at present. Decreasing and precisely quantifying the detection noise in the future experiments will be necessary to prove that sub-Poissonian number fluctuations are indeed present in our system. If so, further studies of entanglement will become possible [30–32].

Our experiment demonstrates the emission of matter-wave jets from a self-trapped BEC (soliton) due to the modulation of interatomic interaction in quasi-1D confinement. In addition to a single-pulse experiment, in which first and second order jets are created, the double-pulse experiment creates two consecutive first order jets, implying a possibility of multiple consecutive jets. With a high enough number of atoms in the initial condensate one could in principle perform the experiment shown in Fig. 1(b, d) with more than two pulses and thereby create a pulsed atom laser with two correlated beams, a powerful new tool for precision measurements. In multi-pulse experiments new, irregular jets emerge, indicating that in some cases the confinement does not define the direction of the jets, which merits further investigation. Furthermore, we show that a relatively simple numerical calculation fully predicts the qualitative behaviour of the jets and additionally shows the emergence of density waves before jet emission. The simplified 1D geometry removes the angular complexity of previous 2D experiments, making further analysis more straightforward, as exemplified by the number correlation measurements. The results indicate possible sub-Poissonian number fluctuations, which at present remains obscured by the detection noise. In further work an improved imaging system should provide a clearer insight into number squeezing and possible entanglement of jet pairs.

We thank Philipp Haslinger, Stephanie Manz, Lev Vidmar and Andrej Zorko for their helpful comments. We would also like to thank Samo Beguš and Davorin Kotnik

for their help with electronics. This work was supported by the Slovenian Research Agency (research core Grants No. P1-0125 and No. P1-0099, and research project No. J2-8191).

* tadej.meznarsic@ijs.si

† peter.jeglic@ijs.si

- [1] S. E. Pollack, D. Dries, R. G. Hulet, K. M. F. Magalhães, E. A. L. Henn, E. R. F. Ramos, M. A. Caracanhas, and V. S. Bagnato, *Phys. Rev. A* **81** (2010), 10.1103/physreva.81.053627.
- [2] P. Engels, C. Atherton, and M. A. Hoefer, *Phys. Rev. Lett.* **98** (2007), 10.1103/physrevlett.98.095301.
- [3] J. Nguyen, M. Tsatsos, D. Luo, A. Lode, G. Telles, V. Bagnato, and R. Hulet, *Phys. Rev. X* **9** (2019), 10.1103/physrevx.9.011052.
- [4] A. Eckardt, *Rev. Mod. Phys.* **89** (2017), 10.1103/revmodphys.89.011004.
- [5] L. W. Clark, A. Gaj, L. Feng, and C. Chin, *Nature* **551**, 356 (2017).
- [6] H. Fu, L. Feng, B. M. Anderson, L. W. Clark, J. Hu, J. W. Andrade, C. Chin, and K. Levin, *Phys. Rev. Lett.* **121** (2018), 10.1103/physrevlett.121.243001.
- [7] L. Feng, J. Hu, L. W. Clark, and C. Chin, *Science* **363**, 521 (2019).
- [8] T. Chen and B. Yan, *Phys. Rev. A* **98** (2018), 10.1103/physreva.98.063615.
- [9] M. Arratia, *J. Phys. B: At., Mol. Opt. Phys.* **52**, 055301 (2019).
- [10] Z. Wu and H. Zhai, <http://arxiv.org/abs/1804.08251v2>.
- [11] C. Chin, R. Grimm, P. Julienne, and E. Tiesinga, *Rev. Mod. Phys.* **82**, 1225 (2010).
- [12] Further details of the procedure are described in our previous work [33].
- [13] K. E. Strecker, G. B. Partridge, A. G. Truscott, and R. G. Hulet, *Nature* **417**, 150 (2002).
- [14] L. Khaykovich, F. Schreck, G. Ferrari, T. Bourdel, J. Cubizolles, L. D. Carr, Y. Castin, and C. Salomon, *Science* **296**, 1290 (2002).
- [15] S. L. Cornish, S. T. Thompson, and C. E. Wieman, *Phys. Rev. Lett.* **96**, 170401 (2006).
- [16] J. H. Nguyen, P. Dyke, D. Luo, B. A. Malomed, and R. G. Hulet, *Nat. Phys.* **10**, 918 (2014).
- [17] G. D. McDonald, C. C. N. Kuhn, K. S. Hardman, S. Bennetts, P. J. Everitt, P. A. Altin, J. E. Debs, J. D. Close, and N. P. Robins, *Phys. Rev. Lett.* **113**, 013002 (2014).
- [18] S. Lepoutre, L. Fouché, A. Boissé, G. Berthet, G. Salomon, A. Aspect, and T. Bourdel, *Phys. Rev. A* **94**, 053626 (2016).
- [19] J. H. V. Nguyen, D. Luo, and R. G. Hulet, *Science* **356**, 422 (2017).
- [20] P. J. Everitt, M. A. Sooriyabandara, M. Guasoni, P. B. Wigley, C. H. Wei, G. D. McDonald, K. S. Hardman, P. Manju, J. D. Close, C. C. N. Kuhn, S. S. Szigeti, Y. S. Kivshar, and N. P. Robins, *Phys. Rev. A* **96**, 041601 (2017).
- [21] Using the nomenclature from [7], J1 would be the first ring and J2 the 4th ring.
- [22] H. Miesner, D. M. Stamper-Kurn, M. R. Andrews, D. S. Durfee, S. Inouye, and W. Ketterle, *Science* **279**, 1005 (1998).
- [23] L. Salasnich, A. Parola, and L. Reatto, *Phys. Rev. Lett.* **91** (2003), 10.1103/physrevlett.91.080405.
- [24] We used the split-step spectral method to solve for the real-time dynamics of the BEC on a 1D grid of 32768 points in the interval [-800:800] with time-step $\tau = 0.001$.
- [25] R. Bücker, J. Grond, S. Manz, T. Berrada, T. Betz, C. Koller, U. Hohenester, T. Schumm, A. Perrin, and J. Schmiedmayer, *Nat. Phys.* **7**, 608 (2011).
- [26] C. Gross, H. Strobel, E. Nicklas, T. Zibold, N. Bar-Gill, G. Kurizki, and M. K. Oberthaler, *Nature* **480**, 219 (2011).
- [27] B. Lücke, M. Scherer, J. Kruse, L. Pezze, F. Deuretzbacher, P. Hyllus, O. Topic, J. Peise, W. Ertmer, J. Arlt, L. Santos, A. Smerzi, and C. Klempt, *Science* **334**, 773 (2011).
- [28] M. Bonneau, J. Ruauudel, R. Lopes, J.-C. Jaskula, A. Aspect, D. Boiron, and C. I. Westbrook, *Phys. Rev. A* **87** (2013), 10.1103/physreva.87.061603.
- [29] E. M. Bookjans, C. D. Hamley, and M. S. Chapman, *Phys. Rev. Lett.* **107** (2011), 10.1103/physrevlett.107.210406.
- [30] M. Fadel, T. Zibold, B. Décamps, and P. Treutlein, *Science* **360**, 409 (2018).
- [31] P. Kunkel, M. Prüfer, H. Strobel, D. Linneemann, A. Frölian, T. Gasenzer, M. Gärttner, and M. K. Oberthaler, *Science* **360**, 413 (2018), <https://science.sciencemag.org/content/360/6387/413.full.pdf>.
- [32] K. Lange, J. Peise, B. Lcke, I. Kruse, G. Vitagliano, I. Apellaniz, M. Kleinmann, G. Tóth, and C. Klempt, *Science* **360**, 416 (2018).
- [33] T. Mežnaršič, T. Arh, J. Brence, J. Pišljari, K. Gosar, Ž. Gosar, R. Žitko, E. Zupanič, and P. Jeglič, *Phys. Rev. A* **99** (2019), 10.1103/physreva.99.033625.